# MEASUREMENTS OF THE ELECTRON CLOUD IN THE APS STORAGE RING

K. C. Harkay [#] and R. A. Rosenberg, Advanced Photon Source
Argonne National Laboratory, Argonne, IL 60439 USA

*Abstract*

Synchrotron radiation interacting with the vacuum chamber walls in a storage ring produce photoelectrons that can be accelerated by the beam, acquiring sufficient energy to produce secondary electrons in collisions with the walls. If the secondary-electron yield (SEY) coefficient of the wall material is greater than one, as is the case with the aluminum chambers in the 7-GeV Advanced Photon Source (APS) storage ring, a runaway condition can develop. As the electron cloud builds up along a train of stored positron or electron bunches, the possibility exists that a transverse perturbation of the head bunch will be communicated to trailing bunches due to interaction with the cloud. In order to characterize the electron cloud, a special vacuum chamber was built and inserted into the ring. The chamber contains 10 rudimentary electron-energy analyzers, as well as three targets coated with different materials. Measurements show that the intensity and electron energy distribution are highly dependent on the temporal spacing between adjacent bunches and the amount of current contained in each bunch. Furthermore, measurements using the different targets are consistent with what would be expected based on the SEY of the coatings. Data for both positron and electron beams are presented.

## 1 MOTIVATION

Postulation of an electron-cloud instability (ECI) arose from observations with stored positron beams at the KEK Photon Factory [1]. Similar results were later obtained at BEPC [2] and possibly at CESR [3]. Theoretical simulations predict large amplitude motions produced in the tail of positron bunch trains, leading to beam loss [4]. Although results from the models are consistent qualitatively with the observations, the electrons had not been directly measured. The goal of the measurements at the APS storage ring is to characterize the electron cloud (EC) so as to better predict conditions leading to a possible electron-cloud instability. Of particular interest is to provide realistic limits on critical input parameters in the models: the SEY of different surfaces in a real chamber and the influence of single or multiple reflections of the photons.

## 2 EXPERIMENTAL SETUP

In order to measure the properties of the electron cloud, a special 5-m vacuum chamber, equipped with rudimentary electron energy analyzers, beam position monitors (BPMs) and targets, was built and installed in a field-free region in the APS storage ring [5] in May 1998. The locations of the components are shown in Fig. 1. EA6 is a copper end absorber designed to intercept high-energy photons to protect the downstream surfaces. Given that the chamber is straight, the bending magnet synchrotron radiation fan penetrates slightly farther into the channel at the downstream detectors.

The electron detector consists of two mesh grids in front of a collector: the outermost grid is grounded, and a bias voltage can be applied to the shielded grid. The collector is graphite-coated to lower the secondary-electron yield (SEY) and is biased at +45 V with a battery to maximize its collection efficiency. The average detector resolution is 4% fwhm, measured using 100-eV electrons from an electron gun.

The detectors are mounted on a 2-3/4 in. flange on a standard-aperture vacuum chamber as close to directly opposite the antechamber channel as its geometry will allow, as shown in Fig. 1. The channel allows most of the high-energy photons to escape without interacting with the chamber walls. The penetration into the vacuum chamber for the detectors was slotted for rf shielding and coupling impedance considerations. A standard BPM is mounted opposite a detector at three locations for comparison. The BPM surface area and the detector aperture are both ~1 $cm^2$. A removable, water-cooled, target is shown inserted in the channel to the right. Data were collected by measuring the collector current with a picoammeter as a function of bias applied to the retarding grid.

## 3 MEASUREMENTS

Amplification of the electron cloud due to secondary production is expected to be the most serious factor leading to a possible EC instability. Machine studies at the APS storage ring were designed to characterize and distinguish among the various contributions to the electron cloud. For a fixed beam energy, the average total number of photoemitted electrons (PE) will be linear with beam current and independent of the temporal distribution of the beam. This contribution includes photoelectrons and secondaries produced in the collision of the photons with the walls. In the absence of multipactoring effects, the electron density will depend primarily on the distance from the main electron source, the EA6 absorber, and in a minor way on electrons produced by the bending magnet radiation and x-rays that are emitted by fluorescence from EA6. In con-

[#] Email: harkay@aps.anl.gov

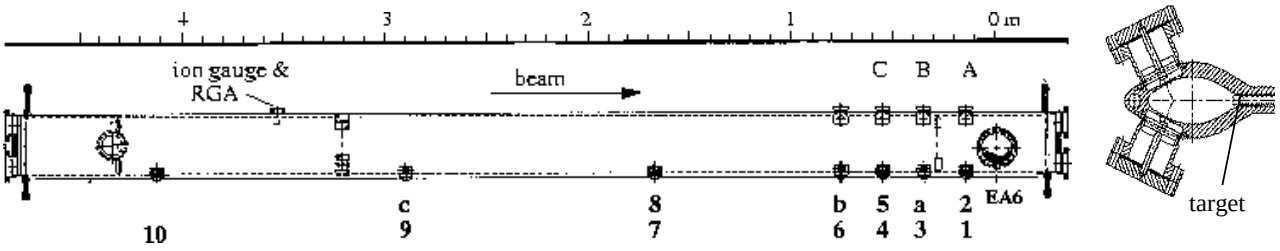


Figure 1: Modified chamber (top view) showing locations of: electron detectors 1-10; BPMs a, b, and c; and targets A, B, and C. On the right is a cross-section schematic showing target and mounting of detectors.

trast, the total number and energy distribution of secondary electrons (SE), produced in collisions with the walls by EC electrons accelerated by the beam, will be highly dependent on the bunch charge and spacing, since this determines the acceleration of the electrons (the SEY is energy-dependent).

## *3.1 Positrons*

A typical measurement of the detector current, normalized to the total beam current, as a function of bias voltage (I-V) is shown in Fig. 2 for four of the detectors. In this example, 20 mA are stored in 10 bunches spaced at 128 rf buckets, or 0.36 μs. The +45 V bias on the collector assures that all the electrons are collected when the bias grid voltage is positive, i.e., the peak of the I-V curve is the total number of electrons integrated over all energies. The normalized electron current at this large spacing is identical to that with a single bunch; therefore, this I-V signature is believed to be determined mostly by the PE.

The dependence on the detector location is seen in Fig. 3. As expected, EA6 is the primary source of electrons, dominating the signal at detectors 1-2 (< 0.3 m). The nearly linear slope of the normalized current at the 128-bucket spacing for detectors 4-9 (> 0.5 m) is consistent with their location.

*Beam-induced Multipactoring*

A **dramatic** amplification of the signal is observed at a 7-bucket bunch spacing (~20 ns), shown in Fig. 3. This can be attributed to the SE contribution. Detectors 6-9 (>1.4 m from EA6) show a higher amplification, which we speculate comes from multiple scattering of electrons originating from the absorber. A scan in the bunch spacing (10 bunches total) gives a peak in the normalized electron current at a spacing between 8-10 buckets, shown in Fig. 4. In addition, there is a factor of 2.6 increase in the normalized electron current when increasing the beam current from 10 to 20 mA, although the position of the peak remains roughly constant. A fine scan between 1-10 bucket spacing reveals sharp peaks at 7 and possibly 9, shown in the insert. A beam instability, likely unrelated to ECI, limited the bunch current at short spacings. Figures 3 and 4 give evidence of a beam-induced multipactoring effect [6]; the bunch spacing at the peak current equals the wall-to-wall time-of-flight in the vertical direction (full height 42 mm) of electrons with an average energy of 8-12 eV.

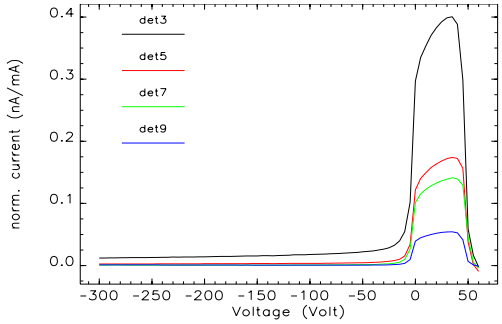


Figure 2: Normalized detector current vs. bias voltage for 10 bunches spaced by 128 buckets.

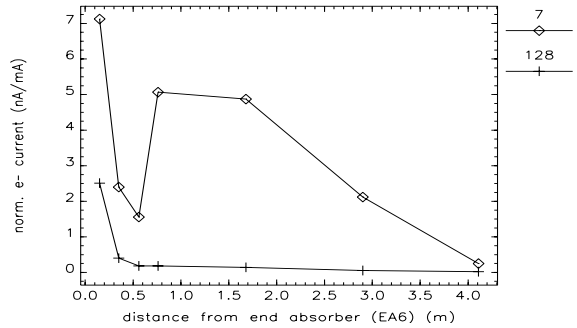


Figure 3: Total, normalized electron current per detector vs. distance from EA6 as a function of bunch spacing (10 bunches, 20 mA).

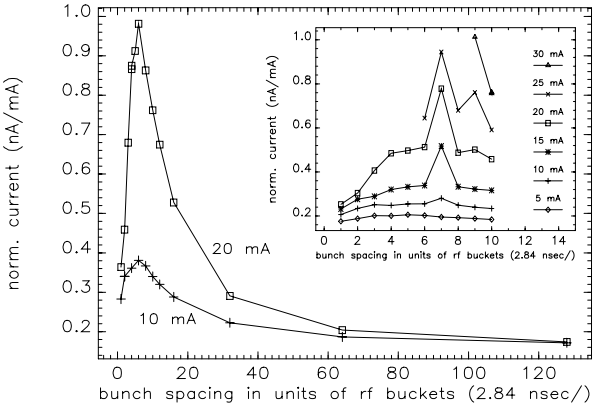


Figure 4: Comparison of normalized electron current as a function of bunch spacing and current (10 bunches total).

The electron energy distribution is dominated by low-energy electrons, seen in the derivative of the I-V curves (Fig. 5). The derivatives have been normalized to high-

light the differences in the energy distributions. The bunch spacing affects the shape of the high-energy tail, giving a longer tail for the multipactoring conditions.

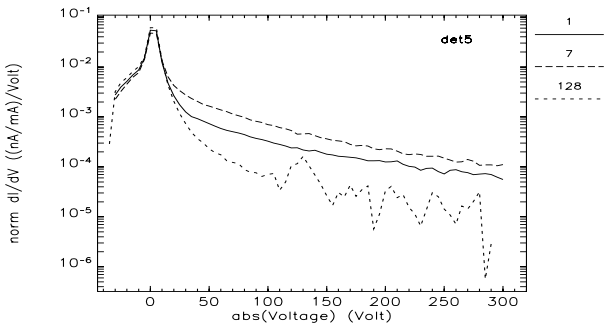


Figure 5: Electron energy distribution vs. bunch spacing.

The buildup of the EC was measured for bunch trains of varying lengths. As expected, the buildup was most pronounced at the 7-bucket spacing, and the most dramatic increases occurred for detectors farthest from EA6. Figure 6 shows the normalized current for detector 9 for bunch trains of varying length, with 1-2 mA/bunch. The total amplification at 2 mA/bunch is a factor of 360 in normalized current, and 50 times higher still in absolute electron current. A pressure rise of a factor of 20 was observed for these conditions over the pressure without multipactoring (0.5 nTorr), indicative of enhanced desorption induced by the secondary electrons, and giving independent evidence of the multipactoring effect [6]. A saturation effect is observed beyond a certain number of bunches, beyond which the increases becomes linear.

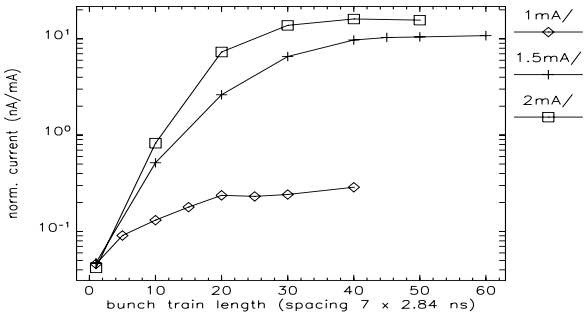


Figure 6: Amplification of EC over bunch trains.

The variation with target SEY was measured by inserting each of the targets (Cu, oxidized Al, and TiN) separately. Ratios of the detector current at 7-bucket spacing (maximum SE) and 128-bucket spacing (minimum SE) were obtained. The ratio was greatest for Al and about the same for Cu and TiN, which is roughly consistent with the relative SEY. The differences, however, were small, which is to be expected since the surface areas of the targets are small compared to that of the chamber.

The maximum, normalized detector currents decreased over time for the same beam conditions as the walls became conditioned after installation of the chamber. After an integrated current of 62.5 A-h, the PE-dominated signal decreased by 20% and the SE-dominated signal decreased by 45%. This suggests that as the oxidized Al surface becomes more metallic as a result of conditioning, the SEY is lowered, which affects the SE to a greater degree compared to the PE.

### *3.2 Electrons*

Conversion to electrons in Sept. 1998 allowed comparison of the electron cloud data with a positron beam. The results are qualitatively very similar. There is a peak in the normalized electron current with bunch spacing, although it occurs at an 11-bucket spacing. This is not unexpected, as the trajectories of low-energy electrons accelerated by an electron beam will differ from those by a positron beam. The buildup of the electron cloud was also observed over long trains of bunches, with a similar saturation effect. The amplification is more modest: a factor of 14 at 50 bunches with 2 mA/bunch.

## 4 SUMMARY

Dramatic amplification has been observed in the electron cloud in the APS storage ring under certain stored beam conditions. Beam-induced multipactoring effects gave rise to amplification factors up to 18,000 in long positron bunch trains with 2 mA/bunch, spaced at 7 rf buckets (~20 ns). A pressure rise of an order of magnitude was observed for these conditions, over that without multipactoring. More modest amplifications were seen for long electron bunch trains, but at a spacing of 11 buckets. Although the electron cloud instability is not a resonant phenomenon, beam-induced multipactoring appears to be an important effect in the amplification and buildup of the electron cloud. Preliminary results with targets of different materials show a reduction in the SE production for Cu or TiN surfaces compared to oxidized Al. Comparisons of these data with simulations are planned, with the goal of developing an empirical model for realistic chamber geometries. A detailed report is in preparation.

## 5 ACKNOWLEGEMENTS

The authors would like to thank J. Galayda for the inpiration for these studies, and G. Goeppner, J. Gagliano, J. Warren, M. McDowell, and B. Yang for their technical assistance. This work was supported by the U.S. Department of Energy, Office of Basic Energy Sciences, under Contract No. W-31-109-ENG-38.

## 6 REFERENCES

[1] M. Izawa, Y. Sato, T. Toyomasu, Phys. Rev. Lett. 74, 5044 (1995)

[2] Z.Y. Guo et al., Proc. of 1997 PAC, 1566 (1998) and Proc. of 1998 EPAC, 957 (1998)

[3] J.T. Rogers, KEK Proc. 97-17, 42 (Dec. 1997)

[4] K. Ohmi, Phys. Rev. Lett. 75, 1526 (1995)

[5] ANL Report Nos. ANL 87-15 (1987) and ANL/APS/TB-26 (1996)

[6] O. Gröbner, Proc. of 10th Int'l Conf. on High Energy Accel., Protvino, 277 (1977)